Physics and Chemistry of the Earth 83–84 (2015) 28–35

Contents lists available at ScienceDirect

Physics and Chemistry of the Earth

journal homepage: www.elsevier.com/locate/pce

Inferring land surface parameters from the diurnal variability of microwave and infrared temperatures

Hamidreza Norouzi [a,*], Marouane Temimi [b,c], Amir AghaKouchak [d], Marzieh Azarderakhsh [e], Reza Khanbilvardi [b], Gerarda Shields [a], Kibrewossen Tesfagiorgis [f]

[a] New York City College of Technology, The City University of New York, USA
[b] The City College of New York, NOAA-Cooperative Remote Sensing Science and Technology Center (CREST), USA
[c] Masdar Institute of Science and Technology, Abu Dhabi, United Arab Emirates
[d] University of California, Irvine, USA
[e] Fairleigh Dickinson University, USA
[f] Borough of Manhattan Community College, The City University of New York, USA

ARTICLE INFO

Article history:
Received 22 September 2014
Received in revised form 21 January 2015
Accepted 31 January 2015
Available online 27 February 2015

Keywords:
Microwave brightness temperature
Diurnal amplitude
Phase lag
Soil texture
Land surface temperature
Land cover

ABSTRACT

This study investigates the properties of the diurnal cycle of microwave brightness temperatures (TB), namely the phase and the amplitude, and their variability in time and space over the globe to infer information on key land surface parameters like changes in soil texture spatial distribution, soil moisture conditions, and vegetation density. The phase corresponds to the lag between Land Surface Temperature (LST) and TB diurnal cycles. The amplitude is determined as the difference between the maximum and the minimum of TB diurnal cycle. The diurnal cycle of TB was constructed using observations from the Advanced Microwave Scanning Radiometer-Earth Observing System (AMSR-E) and the Special Sensor Microwave/Imager (SSM/I). The latter offer a series of sensors, namely, F13, F14, and F15 that were used in this study for a higher temporal coverage and more accurate diurnal cycle determination. LST estimates, which are available every 3 h from the International Satellite Cloud Climatology Project (ISCCP) database were used to build the LST diurnal cycle. ISCCP LST data is an infrared-based temperature with almost no penetration and is the representative of top skin temperature.

The analyses of the diurnal cycles showed that the diurnal amplitude of TB decreases as the vegetation density increases, especially in the case of low frequencies which penetrate deeper into the canopy which makes them more sensitive to changes in vegetation density. The interannual variations of TB diurnal amplitudes were also in agreement with the seasonality of the vegetation cover. Over desert and rain forest regions where surface conditions do not vary significantly throughout the year, the changes in diurnal amplitudes were the lowest. A relationship between phase and amplitude values was established. It was found that the amplitude of TB diurnal cycle decreases when the phase lag increases. The spatial distribution of the determined diurnal properties, namely, phase and amplitude of TB, showed an agreement with lithology maps in desert areas. Lower TB amplitudes were observed over regions with loose siliceous rocks. Phase lag values between 1.5 and 3 h corresponded to 83% of the class "loose siliceous rocks" in the Sahara Desert, which corroborates the potential of using the diurnal properties of TB as an indicator of land surface parameters.

1. Introduction

Microwave brightness temperature (TB) is sensitive to key surface parameters, such as soil moisture, snow cover, freeze/thaw state, land surface temperature, and vegetation structure (e.g. Min et al., 2010; Njoku et al., 2003; Tedesco and Kim, 2006). The retrieval of these parameters typically requires running a radiative transfer model which uses TB observations from ascending or descending overpasses of a single polar orbiting satellite at the same specific time of the day. Then, the retrieved parameters should only correspond to the state of the land surface at acquisition time. Moreover, the retrieval of land surface parameters using radiative transfer models does not account for the diurnal variability of microwave TB with respect to other variables included

* Corresponding author at: New York City College of Technology, 300 Jay Street, V424, Brooklyn, NY 11201, USA. Tel.: +1 718 260 5410; fax: +1 718 260 5677.
E-mail address: hnorouzi@citytech.cuny.edu (H. Norouzi).

http://dx.doi.org/10.1016/j.pce.2015.01.007
1474-7065/

in the model, like, Land Surface Temperature (LST), assuming a perfect sync between LST and TB may undermine the quality of the retrieval.

Nowadays, the considerable number of operational passive microwave sensors allows us to construct the diurnal cycle of TB and study its variability throughout the day. The diurnal variation of land surface temperature, atmospheric temperature, and water vapor profiles due to solar radiation affects the sensitivity of the microwave signal to other surface parameters, such as soil moisture, soil roughness, and vegetation optical depth (Choudhury, 1993) Relying on TB observations from a constellation of passive microwave sensors should improve our understanding of the diurnal variability of the signal and lead to a better retrieval of land surface parameters.

Operational polar orbiting satellites that are equipped with microwave radiometers provide at least two observations per day in most regions of the globe, except at higher latitudes, where the revisit time is shorter. Therefore, in order to construct the diurnal cycle of TB across the globe, observations from the existing operational satellites, which observe the surface of the Earth at different local times, should be aggregated. Over land, microwave TB is controlled mainly by surface emissivity and physical temperature (Choudhury, 1993). The changes in surface parameters affect land emissivity and physical temperature and, therefore the diurnal properties of TB.

The characteristics of skin temperature diurnal cycles from thermal infrared observations have been investigated using the Principal Component Analysis (PCA) approach (Aires et al., 2004). It was concluded that the first three components represent the diurnal amplitude, the phase, and the daytime duration of the diurnal variation (Aires et al., 2004). On the other hand, passive microwave TB affected by the depth of the originating soil layer that varies with frequency, surface type, soil moisture, and mineral types of the region (Prigent et al., 1999) exhibits a distinct diurnal variability. Grody and Weng (2008) showed that, in some desert regions, the difference between microwave TB at 19 and 37 GHz has a positive sign at 6:00 a.m., but changes to negative at 9:00 a.m., because observations in these frequencies originate from different layers. Recently, Temimi et al. (2014) analyzed the diurnal change in the performance of soil moisture retrieval using L-band TB measured throughout the day from a ground based radiometer and stated that the best performance was obtained in early afternoon and that the lowest performance was obtained when early morning TB were used. Prigent et al. (1999) used a physical model based on a semi-infinite heat transfer to simulate the effective temperature variation at different depths. They found that, for some surface types, such as sand dunes in desert regions, microwave temperature has much lower diurnal amplitude compared to the top surface physical temperature variation.

Most of the abovementioned studies were based on observations from SSM/I, which are acquired early in the morning or late in the afternoon. Other sensors, like AMSR-E, which was operational from 2002 to 2011, offered additional observations closer to the daily maxima and minima as the sensor's overpass time over the Equator was around 1:30 a.m./p.m. Along with SSM/I measurements, AMSR-E observations allowed for better apprehension of TB diurnal variability and, therefore, accurately inferring changes in diurnal properties (Norouzi et al., 2012). The purpose of this study is to find the relationship between microwave Tb diurnal characteristics and land cover information and also to compare with skin temperature diurnal cycle using infrared observations. This study adds to previous investigations of diurnal variability of TB through integration of additional TB from AMSR-E and uses the constructed diurnal cycles of TB and LST to intercompare their diurnal parameters with respect to land cover classes on a global scale. The relationship between the diurnal variability of TB and soil texture is investigated, where bare soil conditions are prominent, specifically in desert regions. In addition, this study expands the scope of previous analyses (Aires et al., 2004) and places the focus on both LST and microwave TB diurnal cycles. We argue that the TB diurnal variability with respect to LST at different locations provides relevant information on soil texture and land cover type, particularly in desert areas.

2. Data and methodology

2.1. Background

Assuming that land surface is flat and specular and considering the atmosphere as a non-scattering plane-parallel medium, the emissivity can be written as:

$$Tb_{(p,\upsilon)} = \varepsilon_{(p,\upsilon)} \cdot e^{-\tau(0,H)/\mu} \cdot Ts + (1 - e^{-\tau(0,H)/\mu}) \cdot T^{\downarrow}_{atm} + T^{\uparrow}_{atm} \quad (1)$$

where $\varepsilon_{(p,\upsilon)}$ and $Tb_{(p,\upsilon)}$ are the land surface emissivity and the measured brightness temperatures at polarization p (horizontal, H, or vertical, V) and frequency μ, respectively. Ts is the skin temperature and $T^{\downarrow}_{atm}$ and $T^{\uparrow}_{atm}$ are the downwelling and upwelling brightness temperatures from the atmosphere

After removing the effect of the atmosphere, the land surface TB can be written as (Norouzi et al., 2012):

$$Tb_{(p,\upsilon)} = \varepsilon_{eff_{(p,\upsilon)}} . T_{eff} \quad (2)$$

where T_{eff} is the effective physical temperature and represents the temperature of the layer of soil that is contributing to the radiating microwave signal. Emissivity is a physical parameter, which depends on the characteristics, such as moisture, vegetation, surface roughness, and dielectric constant, as well as the sensor configuration (i.e. viewing angle and frequency). Therefore, for stable surface conditions in time, like in desert or rain forest regions, *TB* diurnal parameters are expected to be persistent and any variation in TB should be the result of changes in T_{eff} in space according to spatial variability of surface conditions. It is worth noting that the changes in T_{eff} that this study is capturing are not necessarily similar with changes in LST, essentially because of differences in the penetration depth that is known as the effective depth. In addition, we assume that surface conditions are stable diurnally. In other words, we expect that the physical and brightness temperatures should vary more rapidly than the surface properties represented by the emissivities over the day. The exceptions are produced by possible land surface variations due to precipitation, soil moisture, dew deposition over vegetated areas, and accumulation of snow.

In radiative transfer modeling, due to the lack of global effective temperature observations, LST is usually utilized to approximate T_{eff}. The penetration of the microwave signal into the soil determines the depth the soil layer is generating the microwave radiations. Over bare soils, the penetration depth should depend on the frequency, the soil texture, the soil temperature profile, and the moisture content. LST, on the other hand, reflects the radiating infrared signal of soil surface skin and unlike the microwave temperature does not penetrate deeper into the soil. The deeper sensing depth of the microwave signal leads to lower amplitude of the TB diurnal cycle and introduces a phase lag between TB and LST diurnal cycles. We expect that the difference between the diurnal cycles of LST and TB that is the result of the difference in their sensing depths and includes valuable information on the changing soil parameters.

To verify this assumption, we propose constructing diurnal cycles from TB and LST measures. Then, we assess the variability of the diurnal cycle of TB globally and analyzed over a number of specific land cover types. A vegetation and land use global data set compiled from a large number of published sources at 1° equal

area grid resolution by Matthews (1983) adopted by Prigent et al. (2001) in 0.25° is used in this study to distinguish between various surfaces types. The classes include rain forest, evergreen forest, deciduous forest, evergreen woodland, deciduous woodland, cultivation, grassland, tundra, shrub land, and desert. The land cover types are global, and the results are determined as an average of the values for each class. In addition, a lithology map of the Sahara Desert and Arabian Peninsula (Jimenez et al., 2010) consisting of 13 different soil texture classes was used to observe the effect of soil texture type on the properties of the microwave TB diurnal cycle.

2.2. Constructing TB and LST diurnal cycles

The AMSR-E L2A product (swath data) is obtained from the National Snow and Ice Data Center (NSIDC). Furthermore, SSM/I observations from the F13, F14, and F15 United States Air Force Defense Meteorological Satellite Program (DMSP) satellites provided by the Global Hydrology Resource Center (GHRC) in gridded format are utilized to construct the diurnal cycle. AMSR-E has six frequencies at 6.925, 10.65, 18.7, 23.0, 36.5, and 89.0 GHz with both horizontal and vertical polarization (Njoku et al., 2003). SSM/I channels, on the other hand, are at 19.25, 22, 37, and 85.5 GHz with both horizontal and vertical polarization except for the 22 GHz channels which is only available in the vertical polarization. Only AMSR-E channels, which are similar to SSM/I channels, are used in this study. Hereafter, these frequencies are called 19, 22, 37, and 89 GHz. TMI sensor also may sound helpful in determining the TB diurnal variation construction. However, the TMI overpass time drifts slowly, which means that the sample size at each time of the day in a month is very small and its spatial coverage is limited to 38°N and 38°S latitudes. Moreover, TMI was shown to have some diurnal biases when compared to other conical sensors such as AMSR-E and SSM/I due to solar heating of its main reflector (Geer et al., 2010). This issue was addressed by Biswas et al. (2010) and was implemented in TMIv7. To avoid possible calibration problems, this study just uses similar channels of AMSR-E and SSM/I that are already inter-calibrated (Holmes et al., 2013b). The particular differences in incidence angle and frequency do not induce any substantial differences in TB from AMSR-E and SSM/I (Norouzi et al., 2011). The diurnal cycle from different sensors are often affected by synoptic variations as well as variations due to calibration differences, re-projection, and differences in sensors configuration.

A total of four passive microwave radiometers, three on DMSP satellites (F13, F14, and F15) and one onboard on Aqua satellite that provides observations from ascending and descending overpasses, are used in this study. Thus, a total of eight observations were available on a daily basis to construct the TB diurnal cycles. The time of observation at each location for all satellites is constant with respect to local solar time because their orbits are sun-synchronous. The overpass times of the three DMSP satellites and AQUA vary between 6:00 and 9:00 a.m./p.m. and 1:30 a.m./p.m. local time. A 4th degree best-fit model has been adopted to fill in the gaps and construct the full diurnal cycle of microwave temperature on a pixel basis over the entire globe. Only cloud free observations are used which reduces the spatial coverage on a given day and produces temporal coverage gaps. Although microwave observations (especially at lower frequencies) are less sensitive to clouds, for consistency reasons a restrictive cloud mask, which includes rainy and cloudy pixels, was used. The cloud mask, which is part of the ISCCP data set, was used to detect cloudy pixels. In addition, gaps between consecutive orbit swaths constitute a further loss of data, which reduces the chance for obtaining 8 clear sky microwave observations per day (less than 10% globally). Therefore, the average of the cloud free observations for each crossing time in a month is used to determine the shape of the monthly mean diurnal cycle at each location. This typical monthly mean diurnal cycle may still have some contamination by synoptic variability (Norouzi et al., 2012). In addition to the analysis of microwave temperatures and constructing their diurnal cycles, surface skin temperatures were also analyzed, and their diurnal cycles were constructed. It was necessary to detect cloudy pixels when building diurnal cycles of microwave and surface skin temperatures. Both surface skin temperature and cloud cover products were obtained from the International Satellite Cloud Climatology Project (ISCCP). The ISCCP-DX data set provides global information on skin temperature and cloud coverage every 3 h at about 30 km spatial resolution since 1983 (Rossow and Schiffer, 1999). Recent studies show that available global skin temperatures have significant differences, generally only a few degrees but up to 20 K in deserts (Jimenez et al., 2011). The diurnal cycle of LST was constructed using an hourly Spline interpolation of 3-hourly estimates of skin temperature from ISCCP LST products (Norouzi et al., 2012).

2.3. Diurnal amplitude and phase lag

In this study, in order to investigate the properties of microwave TB diurnal cycle, the amplitude and the phase lag are defined based on both LST and TB diurnal cycles. The diurnal amplitude is calculated based on the difference between maximum and minimum of constructed TB diurnal cycle using SSM/I and AMSR-E observations.

$$\mathrm{TB}^{\mathrm{Amplitude}}_{(p,v)} = \mathrm{TB}^{\max}_{(p,v)} - \mathrm{TB}^{\min}_{(p,v)} \tag{3}$$

where $\mathrm{TB}^{\mathrm{Amplitude}}_{(p,v)}$ is the monthly average diurnal amplitude at polarization p (horizontal, H, or vertical, V) and frequency μ. $\mathrm{TB}^{\max}_{(p,v)}$ and $\mathrm{TB}^{\min}_{(p,v)}$ are the maximum and minimum brightness temperatures over a day. The timing of the maximum temperature with respect to the timing of occurrence of the peak of LST is also an important factor. Therefore, a phase lag time is proposed as follows:

$$\mathrm{Phase}_{p,v} = t^{\max}_{(p,v)} - t_{\mathrm{LST}} \tag{4}$$

$\mathrm{Phase}_{p,v}$ is the phase lag time between microwave TB and LST diurnal cycles. $t^{\max}_{(p,v)}$ is the occurrence time of maximum TB and t_{LST} is the time of maximum LST based on Spline method on ISCCP data.

3. Results

Fig. 1 depicts the typical anomalies of diurnal variation of microwave TB determined using observations collected in July 2005 over five different land cover types at 19, 22, 37, and 89 GHz (vertical polarization). Anomalies are calculated by removing the mean daily TB from the diurnal variations averaged globally over each land cover type. The five selected land cover classes ranged from densely vegetated rain forest areas to desert regions. Fig. 1 shows that the largest amplitude of the diurnal cycle was associated with desert areas. At the lowest two frequencies, namely the 19 and the 22 GHz, the grassland class showed a similar behavior to desert. The gap between the two classes, desert and grassland, at higher frequencies is larger. The lowest amplitude of TB diurnal cycle across all frequencies was associated with the rain forest land cover type. Like over bare soils in desert, the microwave signal penetrates deeper into the canopy as the frequency decreases, in rain forest are which leads to a decline of the amplitude of the TB diurnal cycle because of the high amounts of vegetation water content, intercepted water, and higher scattering mostly generated by branches and leaves (Lu et al., 2009). The denser the vegetation, according to the land-cover classes, the smaller the diurnal amplitude of TB. In fact, the average values of the diurnal

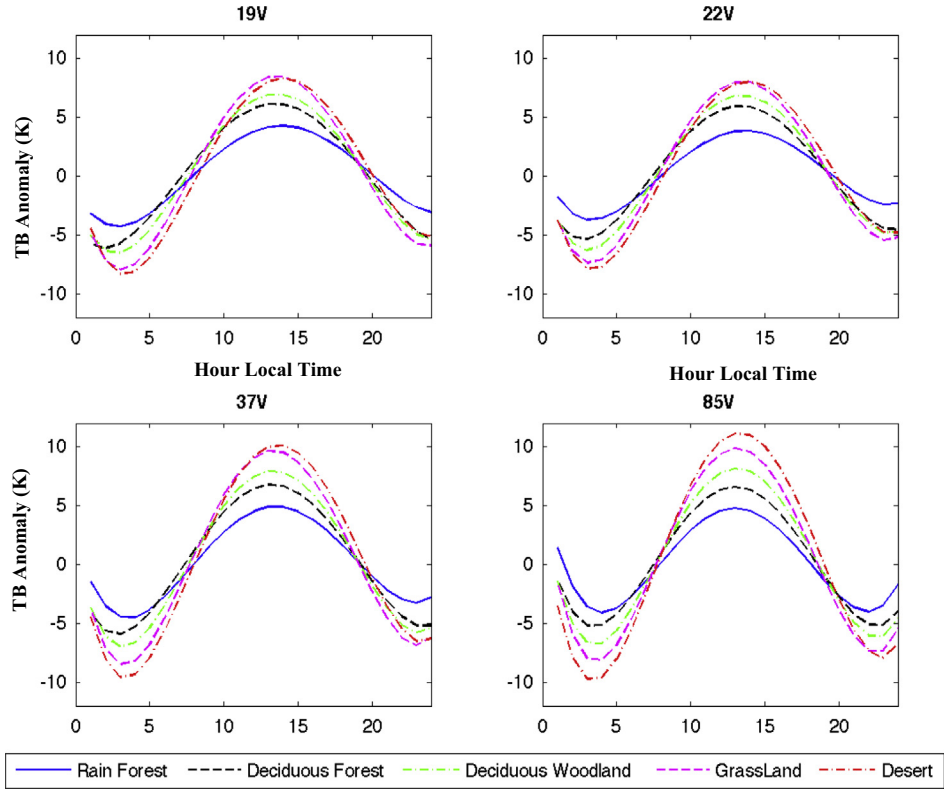

Fig. 1. Anomalies of TB diurnal cycle (K) at different channels for different land vegetation classes (July 2005).

amplitude range from 23 K in desert regions to 8 K in rain forests. Moreover, the variability of the amplitude of the diurnal cycle across the different land classes is more significant at 89 GHz (Fig. 1) than at lower frequencies, such as 19 GHz, where the amplitude does not exhibit a significant change from one class to another. This is because the 89 GHz microwave TB is more sensitive to the top surface, while the 19 GHz microwave observation originates from a deeper layer. Similar results were seen with H polarization microwave TB.

Interannual variability of the diurnal amplitude of TB was analyzed globally from 2003 to 2007 over different land cover types. The results at 19V and 89V GHz, namely, the lowest and highest frequencies onboard SSM/I and AMSRE, respectively, are presented in Fig. 2 to illustrate the interannual variability of low and high frequencies in Northern and Southern hemispheres. The rain forests show the smallest diurnal amplitude with low interannual variability because of the persistency of their vegetation cover throughout the seasons. This land cover type has high moisture amount that causes to dampen the diurnal variation of temperature. The deciduous forest and woodland classes show higher seasonal dynamics because the vegetation density and soil moisture may change seasonally in these regions. However, desert regions, unlike the rest of the analyzed classes, present a typical variability which consists of a low seasonality especially in Northern hemisphere (it has higher seasonality in Southern hemisphere) with high diurnal amplitudes. In Northern hemisphere, the desert regions contain regions with more sand dunes soil, while the southern regions deserts are from rock soils. This may result the differences in heat capacity of the surface and to cause differences in TB diurnal cycle. Moreover, detailed sub-vegetation classes also may exist between two hemispheres. This causes to observe different seasonal trends in same land cover types between two hemispheres. All seasonal analyses in Fig. 2 reveal that diurnal amplitude increases as the vegetation density decreases. For instance average grassland amplitude is higher than deciduous woodland with higher seasonality. The particularity of the variability of microwave TB in desert regions fostered our interest in analyzing the properties of the diurnal cycles and their potential to indicate spatial variability of some soil texture classes across the region. The gap in 2003 is related to lack of enough "clear-sky" observations from all four satellites during a particular month. The increase in 2004 also could be related to inconsistencies among the sensors and the effect of the water vapor diurnal variation or error in cloud and rain masks used in the algorithm. With respect to the inter-channel variability, the magnitude, as shown in Fig. 1, was systematically higher in the 89 GHz than in the 19 GHz across all of the classes. Similar analyses conducted with different observations from different channels (not shown here) showed gradual decline in the magnitude from high to low frequencies.

To investigate the spatial distribution across the globe of the differences in the seasonality of the diurnal amplitude, we mapped diurnal amplitudes of TB at 19 GHz vertical polarization for January and July 2003 in Fig. 3. The results over Sahara desert confirm that TB diurnal amplitude does not exhibit significant seasonal variation, as the pattern of the amplitude remained the same in both seasons. Other stable land cover types such as rain forests also show stable low diurnal amplitude, even lower than desert amplitudes. However, other land cover types with medium vegetation densities present considerable change in TB diurnal amplitude between winter and summer. For instance high latitude regions show a change in TB diurnal amplitude from less than 5 K in winter to more than 15 K in the summer due to vegetation growth and snow existence. Over the desert regions in both seasons, especially in Sahara desert, there are some regions that do not exhibit high diurnal amplitude in TB diurnal cycle. This is in contrasts with infrared-based thermal temperatures that are expected in arid regions (Aires et al., 2004).

In desert regions, microwave TB and LST tend to originate from different depths because the microwave TB penetrates deeper than

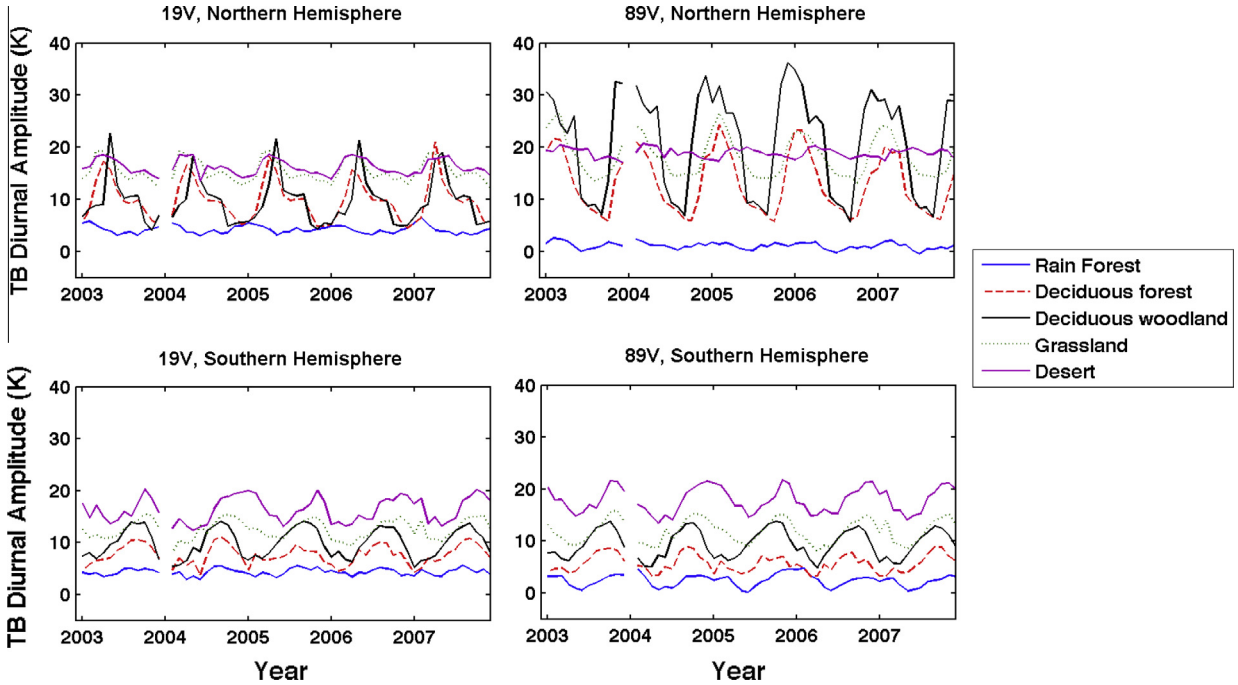

Fig. 2. Interannual variability of microwave TB diurnal amplitude over different land cover types at 89V and 19V GHz for Northern and Southern Hemispheres.

LST due to favorable soil texture and dry conditions. These discrepancies suggest further investigation of the relationship between phase and amplitude of LST and TB in desert regions. The lag time between the occurrence of the maximum of LST and TB is calculated for each pixel in North Africa and Saudi Arabia (latitudes between 10°N and 40°N, and longitudes between 30°W and 60°E). This region is the largest desert area in the world with a variety of soil texture types. The amplitudes of TB diurnal cycles are also calculated based on the difference between maximum and minimum brightness temperature throughout the day in this region. The maps of phase lag and amplitude at 19 GHz (V polarization) are compared to the soil texture map of this region (Fig. 3). There are some regions that have small TB diurnal amplitudes, which is in contrast with typical LST values in desert regions (Aires et al., 2004; Holmes et al., 2013a). Fig. 4 (middle) clearly shows large differences in the timing of the maxima of TB and LST diurnal cycles, up to three hours in certain areas. By examining the lithology map of the Sahara Desert and Arabian Peninsula (Fig. 3 bottom) (Jimenez et al., 2010), one can observe those areas showing high phase lags (up to three hours) and small amplitudes correspond to sand dunes or loose siliceous rocks. Also, it was noticed that those areas where phase differences are between 1.5 and 3 h allowed for detecting around 83% of the class loose siliceous rocks in the Sahara Desert. Jimenez et al. (2010) study used both infrared and microwave emissivities to define the pattern soil texture in Sahara desert, and Holmes et al. (2013a) utilized a different method to distinguish the effect of land cover and soil type on microwave signals. This study suggests that the properties of the diurnal cycle of microwave temperatures could be used as a proxy for land surface conditions and soil texture of sand dunes. The average of the TB amplitude is about 10 K in sand dunes of the Sahara Desert compared to the higher TB diurnal amplitude about 21 K for all other soil type classes.

To investigate the relationship between phase and amplitude, the scatter plot of the determined phase lags and amplitudes at 19 GHz (H polarization) is plotted in Fig. 5. The figure clearly depicts that, as the diurnal amplitude of microwave TB decreases, longer phase lag time is observed between the diurnal cycles of LST and TB. The scatter plot also presents two different clusters, one at around zero lag time between LST and TB, and the other one with almost 3 h lag time and about 12 K lower amplitude, which corresponds to loose siliceous rocks, favorable for deeper penetration of the microwave TB signal and the volume scattering. The correlation between the phase lag and amplitude of TB diurnal cycle for 19 GHz (H polarization) was found to be about 76%. The results of decreasing amplitude with increasing phase lag time are consistent with theoretical approach to calculate the temperature diurnal cycle for a given depth and time of the day using the first two terms of the Fourier (Prigent et al., 1999).

The regression between the phase and amplitude was examined in different months (not shown in the paper) and showed similar trends to the regression obtained for the January data and similar agreement with the lithology map. This consistency supports the use of diurnal cycle properties as indicators of some soil texture classes (sand dune, in particular) regardless of the season. A similar relationship was noticed at higher frequencies but with shorter lag time between LST and TB. A shorter lag time can be explained by closer diurnal variation between TB at higher frequencies and LST because the microwaves at these frequencies originate from layers closer to the surface. Moreover, similar patterns were seen at both vertical and horizontal polarizations for each frequency because they emanate from the same depth (Norouzi et al., 2012).

4. Discussions

Establishing a relationship between TB amplitudes and the phase lag between diurnal cycles of LST and TB could be useful for gap filling under cloudy conditions where LST cannot be retrieved. It is possible relying on a constellation of microwave sensors, like those used in this study, to build the diurnal cycle of TB and estimate its amplitude since the signal is all-weather capable. A similar approach was pursued by Dong et al. (2009) to determine infrared emissivity, yet their study did not make use of the diurnal properties of TB and LST cycles and was based on regression between multi-frequency microwave and infrared

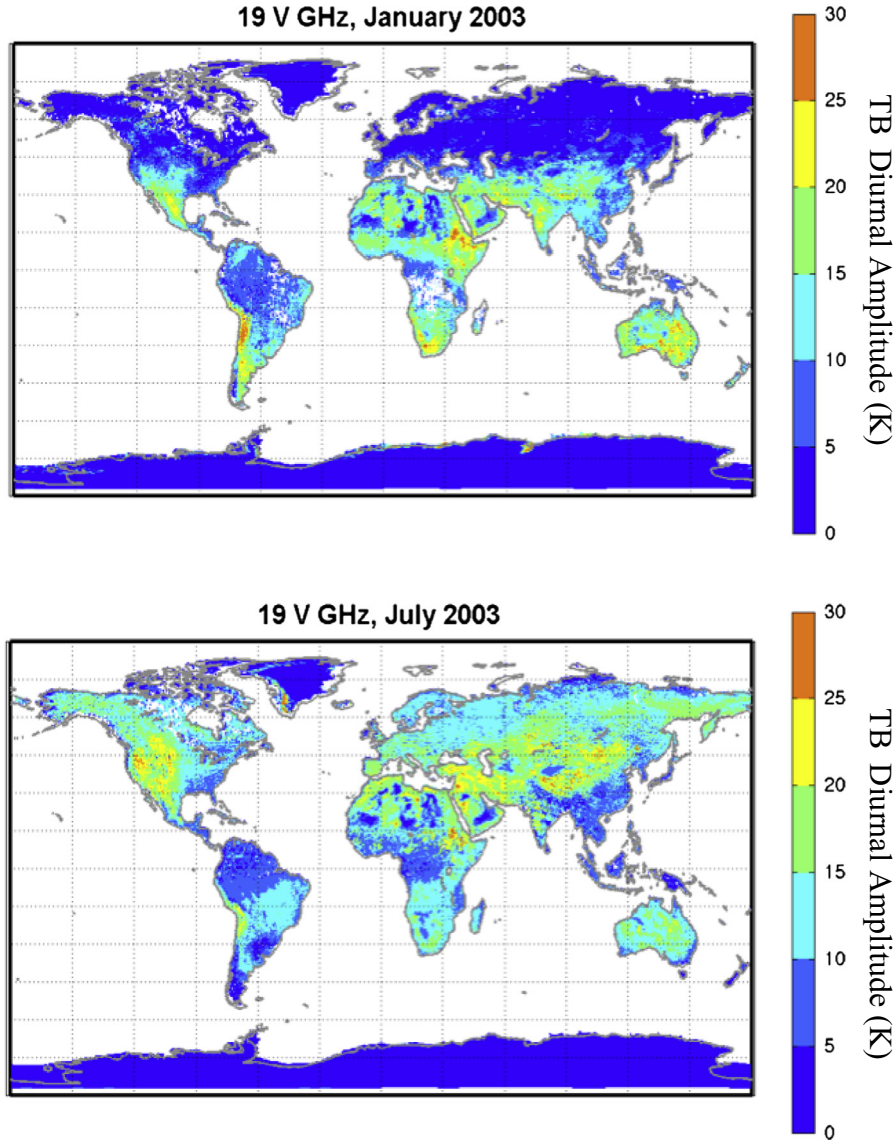

Fig. 3. (Top) TB diurnal cycle amplitude at 19V for January (Top) and July 2003 (Bottom).

emissivity values. This could be investigated and assessed further in future works.

The analysis carried out in this study involved several similar microwave sensors like the SSM/I series. It was assumed that observations from those sensors are consistent if we account for the differences introduced by their overpass times. However, divergences may occur among the sensors and an intercalibration step might be required as it was proposed by Banghua and Fuzhong (2008). The discrepancies can become more significant when observations from sensors (SSMI and AMSR-E) that have different configurations, like altitude and incidence angle, are used together to construct the diurnal cycle of TB. However, we assume in this work that the impact of these possible discrepancies on the overall retrieval of amplitude and phase is minimal. TMI has been used before as a point of reference in inter-satellite consistency analysis that confirms the biases among sensors are less than about 1.0 K (Holmes et al., 2013b).

It is worth noting that this inconsistency between thermal (LST) and microwave brightness temperatures can lead to discrepancies in emissivity retrieval, especially when LST is used as proxy for T_{eff} which may be noticed in emissivity estimates from day/night overpasses (Norouzi et al., 2011, 2012). In stable conditions, in terms of moisture and vegetation, land emissivity should not vary between day and night observations if changes in the atmospheric profiles are neglected. However, the mismatch between thermal and microwave temperatures can introduce an error up to 10% in emissivity retrievals (Norouzi et al., 2012). This issue is more critical in desert regions because of deeper penetration depth of microwave. Previous studies have revealed that in sand loose rock or sand dunes soil type, microwave has the deepest penetration depth and the largest difference with IR diurnal amplitude (Moncet et al., 2011; Norouzi et al., 2012). Therefore, finding this land cover type is much more critical than other land cover and soil texture types in emissivity retrievals. In other land cover types with more vegetation, the difference between IR and microwave TB is less and causes less difference in instantaneous emissivity estimates. These findings demonstrate the necessity of addressing this inconsistency in order to improve the retrieval of land emissivity over sand dunes soil types in deserts (Moncet et al., 2011). The revised effective temperature can be found by the diurnal variation of TB and the average of LST (Norouzi et al., 2012). The discrepancies between LST and TB diurnal cycles can also affect the retrieval of

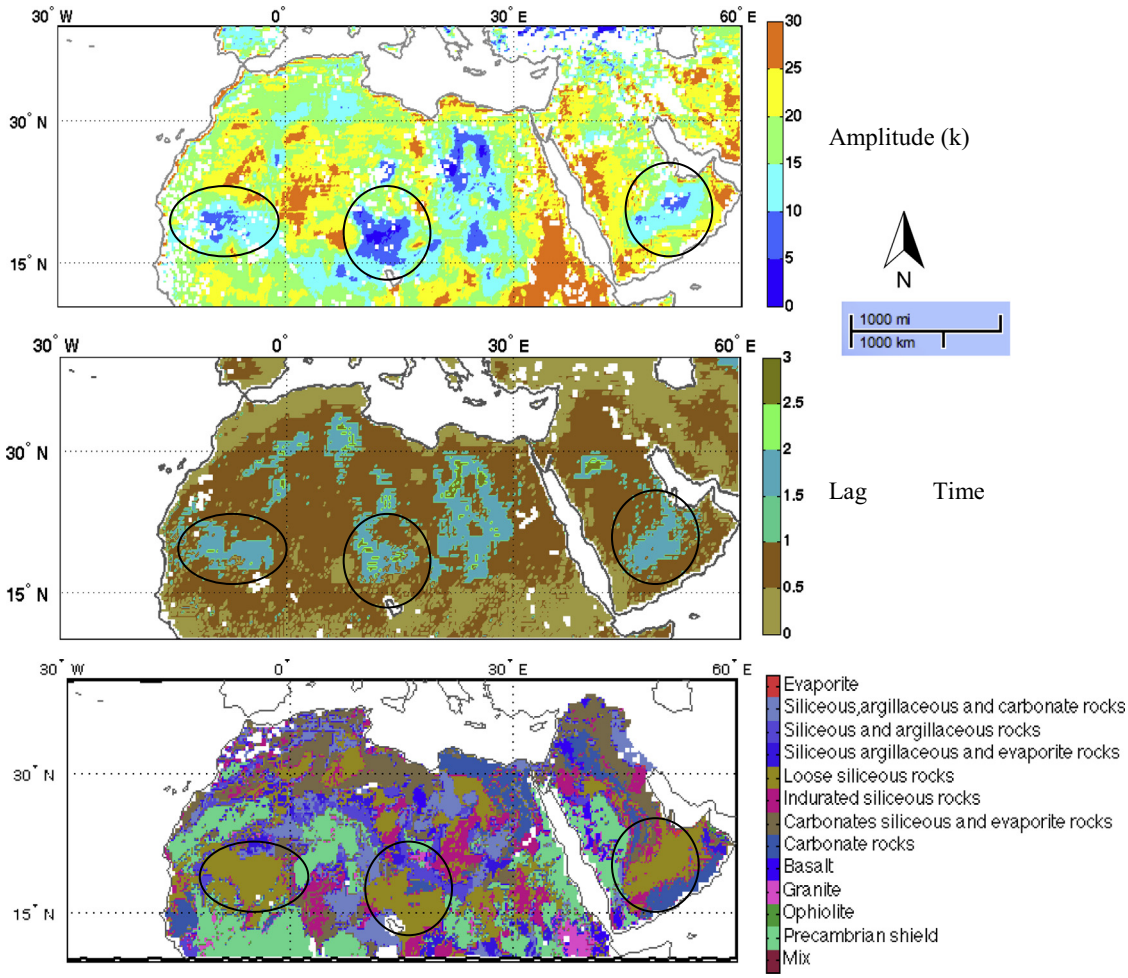

Fig. 4. (Top) TB diurnal cycle amplitude at 19V for July 2003; (Middle) The lag time between skin temperature and TB diurnal cycle at 19V for July 2003 compared to Lithology map (Bottom from Jimenez et al. (2010)) of Sahara Desert and Arabian Peninsula.

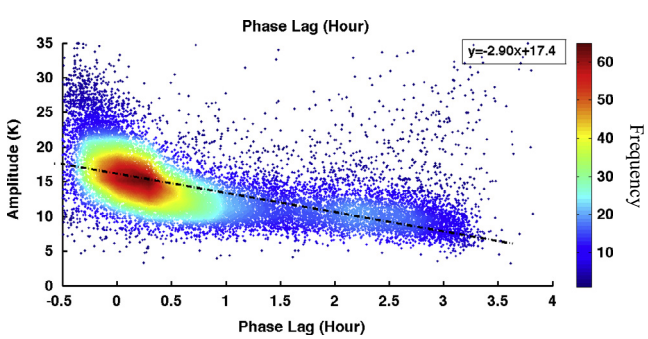

Fig. 5. The relationship between phase lag of LST and TB diurnal cycles and amplitude of microwave TB diurnal cycle at 19 GHz (H polarization) for January 2003 at North Africa Sahara Desert and Arabian Peninsula.

soil moisture (e.g., Soil Moisture Active and Passive (SMAP) mission). The results of this study can be used to account for such discrepancies.

5. Conclusions

In this paper, diurnal cycles of microwave TB and LST were constructed using AMSR-E and SSM/I observations at similar channels and input from the ISCCP database, respectively. The method used in this study benefits from data fusion of microwave observations from multiple sensors which would provide valuable information about earth surface and atmosphere. First, the analysis of the amplitude of the diurnal cycles was done over different land classes across the globe. Strong frequency dependency was found in the diurnal amplitude of microwave temperature because the high frequencies showed greater diurnal amplitude with smaller penetration depth.

The study of TB diurnal variation at different land cover types confirmed that, in highly vegetated areas, the diurnal amplitude is smaller, and deserts have the greatest diurnal variation, except places with sand dunes. Desert and rain forest regions showed small interannual variations compared to other classes with more varying surface conditions. Then, a particular focus was placed on desert regions where surface conditions tend to be more static. The intercomparison of the properties of both TB and LST diurnal cycles seems to provide information on the spatial distribution of soil texture of sand dunes. An analysis of the phase lag between thermal and microwave brightness temperatures showed large differences (up to 3 h) in places where soil texture is favorable for deeper penetration. This led to the mapping of 83% of the loose siliceous rocks class in the Sahara Desert, which corroborates the potential of using diurnal properties as an indicator of some soil types, regardless of the season.

The diurnal variation of TB, derived in this study, can be used in a variety of studies, including reducing systematic errors (AghaKouchak et al., 2012) and uncertainties (AghaKouchak

et al., 2009) observed in satellite precipitation data, analysis of concurrent extremes (e.g., joint precipitation and temperature extremes (Hao et al., 2013)), improving soil moisture (Entekhabi et al., 2010) and snow retrievals, and representation of freeze/thaw in large scale hydrologic studies.

Conflict of interest

There is no conflict of interest.

References

AghaKouchak, A., Nasrollahi, N., Habib, E., 2009. Accounting for uncertainties of the TRMM satellite estimates. Remote Sens. 1 (3), 606–619.

AghaKouchak, A., Mehran, A., Norouzi, H., Behrangi, A., 2012. Systematic and random error components in satellite precipitation data sets. Geophys. Res. Lett. 39 (9), L09406.

Aires, F., Prigent, C., Rossow, W.B., 2004. Temporal interpolation of global surface skin temperature diurnal cycle over land under clear and cloudy conditions. J. Geophys. Res. – Atmos. 109 (D4).

Banghua, Y., Fuzhong, W., 2008. Intercalibration between special sensor microwave imager/sounder and special sensor microwave imager. IEEE Trans. Geosci. Remote Sens. 46 (4), 984–995.

Biswas, S.K., Gopalan, K., Jones, W.L., Bilanow, S., 2010. Correction of time-varying radiometric errors in TRMM microwave imager calibrated brightness temperature products. Geosci. Remote Sens. Lett., IEEE 7 (4), 851–855.

Choudhury, B.J., 1993. Reflectivities of selected land-surface types at 19 and 37 GHz from SSM/I observations. Remote Sens. Environ. 46 (1), 1–17.

Dong, P., Weng, F., Liu, Q., Xue, J., 2009. Deriving infrared land surface emissivity from the Special Sensor Microwave Imager/Sounder. Int. J. Remote Sens. 30 (8), 2021–2031.

Entekhabi, D. et al., 2010. The soil moisture active passive (SMAP) mission. Proc. IEEE 98 (5), 704–716.

Geer, A.J., Bauer, P., Bormann, N., 2010. Solar biases in microwave imager observations assimilated at ECMWF. IEEE Trans. Geosci. Remote Sens. 48 (6), 2660–2669.

Grody, N.C., Weng, F., 2008. Microwave emission and scattering from deserts: theory compared with satellite measurements. IEEE Trans. Geosci. Remote Sens. 46 (2), 361–375.

Hao, Z., AghaKouchak, A., Phillips, T.J., 2013. Changes in concurrent monthly precipitation and temperature extremes. Environ. Res. Lett. 8 (3), 034014.

Holmes, T., Crow, W.T., Hain, C., 2013a. Spatial patterns in timing of the diurnal temperature cycle. Hydrol. Earth Syst. Sci. 17 (10), 3695–3706.

Holmes, T., Crow, W.T., Tugrul Yilmaz, M., Jackson, T.J., Basara, J.B., 2013b. Enhancing model-based land surface temperature estimates using multiplatform microwave observations. J. Geophys. Res.: Atmos. 118 (2), 577–591.

Jimenez, C., Catherinot, J., Prigent, C., Roger, J., 2010. Relations between geological characteristics and satellite-derived infrared and microwave emissivities over deserts in northern Africa and the Arabian Peninsula. J. Geophys. Res. – Atmos. 115.

Jimenez, C. et al., 2011. Global intercomparison of 12 land surface heat flux estimates. J. Geophys. Res. – Atmos. 116.

Lu, S., Ju, Z.Q., Ren, T.S., Horton, R., 2009. A general approach to estimate soil water content from thermal inertia. Agric. For. Meteorol. 149 (10), 1693–1698.

Temimi, Marouane, Lakhankar, T., Zhan, Xiwu, Cosh, Mike, Krakauer, Nir, Kelly, Victoria, Kumissi, Laetitia, 2014. A ground based L band radiometer for the monitoring of soil moisture in the region of Millbrook, New York, USA. Vadose Zone J.

Matthews, E., 1983. Global vegetation and land-use data-bases for climate studies. Bull. Am. Meteorol. Soc. 64 (7), 793–794.

Min, Q.L., Lin, B., Li, R., 2010. Remote sensing vegetation hydrological states using passive microwave measurements. IEEE J. Sel. Top. Appl. Earth Obs. Remote Sens. 3 (1), 124–131.

Moncet, J., Liang, P., Galantowicz, A., Lipton, A., Uymin, G., Prigent, C., Grassotti, C., 2011. Land surface microwave emissivities derived from AMSR-E and MODIS measurements with advanced quality control. J. Geophys. Res. – Atmos. 116.

Njoku, E.G., Jackson, T.J., Lakshmi, V., Chan, T.K., Nghiem, S.V., 2003. Soil moisture retrieval from AMSR-E. IEEE Trans. Geosci. Remote Sens. 41 (2), 215–229.

Norouzi, H., Temimi, M., Rossow, W.B., Pearl, C., Azarderakhsh, M., Khanbilvardi, R., 2011. The sensitivity of land emissivity estimates from AMSR-E at C and X bands to surface properties. Hydrol. Earth Syst. Sci. 15 (11), 3577–3589.

Norouzi, H., Rossow, W., Temimi, M., Prigent, C., Azarderakhsh, M., Boukabara, S., Khanbilvardi, R., 2012. Using microwave brightness temperature diurnal cycle to improve emissivity retrievals over land. Remote Sens. Environ. 123, 470–482.

Prigent, C., Rossow, W.B., Matthews, E., Marticorena, B., 1999. Microwave radiometric signatures of different surface types in deserts. J. Geophys. Res. – Atmos. 104 (D10), 12147–12158.

Prigent, C., Aires, F., Rossow, W., Matthews, E., 2001. Joint characterization of vegetation by satellite observations from visible to microwave wavelengths: a sensitivity analysis. J. Geophys. Res. – Atmos. 106 (D18), 20665–20685.

Rossow, W.B., Schiffer, R.A., 1999. Advances in understanding clouds from ISCCP. Bull. Am. Meteorol. Soc. 80 (11), 2261–2287.

Tedesco, M., Kim, E.J., 2006. Retrieval of dry-snow parameters from microwave radiometric data using a dense-medium model and genetic algorithms. IEEE Trans. Geosci. Remote Sens. 44 (8), 2143–2151.